MECHANICAL PROPERTIES OF AlSi10Mg ALLOY PROCESSED BY SLM

Libor Pantělejev[1,*], Roman Štěpánek[1], Daniel Koutný[2], David Paloušek[2]

[1] Institute of Materials Science and Engineering, NETME centre, Faculty of Mechanical Engineering, Brno University of Technology, Technická 2, 616 69, Brno, Czech Republic
[2] Institute of Machine and Industrial Design, NETME centre, Faculty of Mechanical Engineering, Brno University of Technology, Technická 2, 616 69, Brno, Czech Republic

[*]corresponding author: e-mail: pantelejev@fme.vutbr.cz, tel.: +420 541143188

Resume
The paper deals with mechanical properties of AlSi10Mg aluminium alloy processed by the selective laser melting (SLM) technique. The influence of surface quality and building orientation of the samples on mechanical properties was evaluated. It was found that orientation of the samples had no effect on tensile properties (UTS, 0.2% proof stress) whereas surface quality had a significant effect. An 11% increase in ultimate tensile strength was found in the case of samples of lower surface roughness, and an increase of almost factor two in elongation at break was found for machined samples in comparison to as-built samples.

Article info
Article history:
Received 14 December 2017
Accepted 09 February 2018
Online 10 February 2018

Keywords:
AlSi10Mg;
SLM;
Microstructure;
Mechanical properties;
Fracture behaviour

Available online: http://fstroj.uniza.sk/journal-mi/PDF/2017/14-2017.pdf

ISSN 1335-0803 (print version)
ISSN 1338-6174 (online version)

1. Introduction

Today, when demands for fast production of parts of complex shapes tend to increase, the additive manufacturing technologies (AM) are in the centre of interest [1]. One of the most widely used technologies is Selective Laser Melting (SLM); during this process the final shape of component is manufactured by selective melting of powder material layer by layer [2, 3]. Aluminium alloys are used in automotive and aircraft industries mostly for their high specific strength, thus the manufacturing of components by SLM technology and its optimization are really demanded. The processing parameters (laser power (Lp), laser speed (Ls), hatch distance (Hd) or layer thickness (Lt)) play a significant role in the final properties of SLM processed materials. Inappropriate combination of parameters could result in a major decrease of mechanical properties compared with conventionally fabricated materials, caused by the occurrence of a high amount of defects in the microstructure. The complex analysis of the influence of individual parameters on the final microstructure results in the so-called processing window, which is optimal for specific materials [4, 5]. The most common defect in materials processed by AM is porosity. The origin of pores could be defined by a proper identification of its type [3, 6]. Porosity in the form of spherical cavities (gas-induced porosity) is caused by gas induced into molten metal or transferred into the material already with the powder created during the gas atomization process [7, 8]. In case that the level of introduced energy is not sufficient (lack of fusion) and the metal powder is melted improperly, irregularly shaped pores of different sizes could be found in the microstructure and non-molten powder particles could be located inside of these pores [4, 5, 9]. On the other

hand, if the level of introduced energy is too high, porosity in the form of keyholes takes place in the material [7]. Another type of porosity is shrinkage porosity, originating due to incomplete metal flow to the required melt region [10, 11]. A significant problem in aluminium alloys processed by laser technology is also their susceptibility to cracking [12 – 14].

Besides the processing parameters, the final properties of material are also influenced by the orientation of processed component in the building chamber (regarding the building direction), scanning strategy [15 – 17] and loading conditions [18]. The aim of the paper is to evaluate the influence of sample orientation (compared to the building platform) in combination with different surface qualities on the mechanical properties of AlSi10Mg alloy.

2. Material and experimental methods

AlSi10Mg alloy processed by the SLM method was used in this work. Material in the form of powder was provided by LPW Technology Ltd. The powder exhibited inhomogeneity in particle size and morphology (Fig. 1), declared range of size was 20 - 63 μm. The morphology of particles was evaluated using a Zeiss Ultra Plus scanning electron microscope (SEM). Chemical composition of the powder is given in Table 1. The SLM 280HL (SLM Solutions Group AG) machine equipped with 400 W ytterbium fibre laser with Gaussian profile was used for sample processing. Inert nitrogen atmosphere was used during powder processing in the building chamber.

Two sets of cylindrical samples were processed for the evaluation of mechanical properties. The samples were SLM processed using the following parameters: laser power (Lp) 350 W, laser (scanning) speed (Ls) 933 mm·s^{-1}, hatch distance (Hd) 170 μm, layer thickness (Lt) 50 μm, chessboard strategy, building platform heating: 120 °C, both sets of samples were built with an angle of 0 and 90° (in relation to the building platform plane - Fig. 2), samples were not heat treated after processing. The gauge length of set A of samples was in as-built state with dimensions of ∅ 5 mm × 25 mm (in horizontal position on Fig. 2), the gauge length of set B of samples was additionally machined to dimensions of ∅ 6 mm × 30 mm (in vertical position on Fig. 2). Microhardness HV 0.1 was measured on the cross sections of clamping heads of samples from both sets after their polishing, using a Leco LM 247AT microhardness tester. Tensile tests were performed using the Zwick Z250 testing machine at room temperature at a loading speed of 2 mm·min^{-1}.

A fractographic analysis of samples broken during tensile tests was performed using a Zeiss Ultra Plus scanning electron microscope.

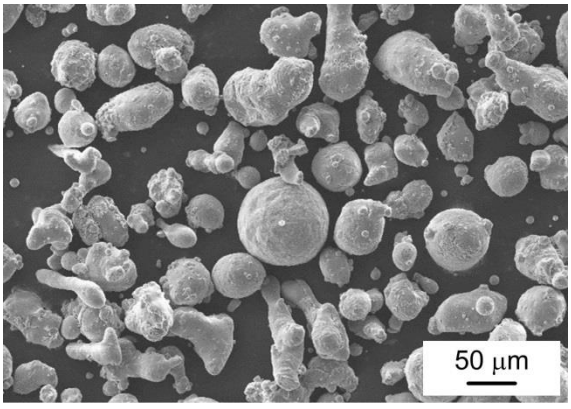

Fig. 1. Morphology and size of powder particles (SEM).

Table 1

Chemical composition of AlSi10Mg powder.

Elements	Al	Si	Mg	Fe	Zn	Cu	Ni	other
Composition, wt. %	balance	10.0	0.4	0.11	<0.1	<0.05	<0.01	<0.37

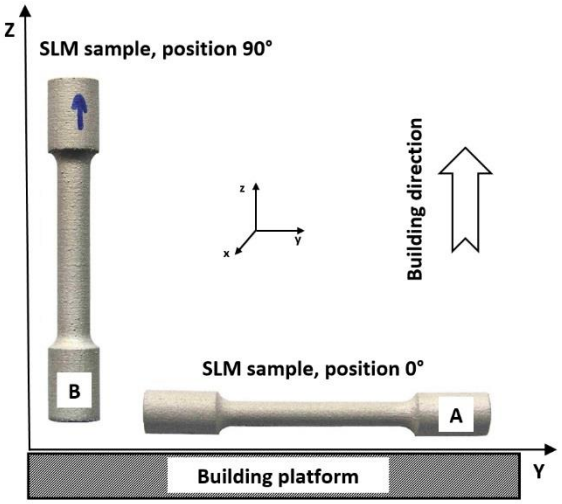

Fig. 2. Built position of samples on building platform.

A metallographic analysis for microstructural evaluation was performed on samples prepared from the clamping head sections of samples from both A and B sets after tensile tests. The plane observed was parallel (samples with a building angle of 0°) and perpendicular (samples with a building angle of 90°) to the building direction. The samples were conventionally prepared using wet grinding, and polished using diamond paste. After etching, the samples were analysed using an Olympus GX 50 light microscope (LM).

3. Results

According to the results of tensile tests (Table 2, Fig. 3) the orientation of samples affects only elongation of both as-built and machined samples. The building direction and surface quality has no influence on 0.2% proof stress but ultimate tensile strength is affected by the surface quality. The average ultimate tensile strength (UTS) of as-built samples is about 45 MPa lower compared with UTS of machined samples. The average microhardness is comparable for both sample orientations, with values of 122 HV 0.1 for 0° orientation and 116 HV 0.1 for 90° orientation (Table 2).

Table 2

Mechanical characteristic for evaluated states.

Sample	Orientation	0.2% proof stress [MPa]	UTS [MPa]	Elongation [%]	Microhardness HV 0.1
as-built	0°	231	377	3.6	116
as-built	90°	242	376	2.7	114
machined	0°	244	423	6.8	128
machined	90°	242	421	4.2	118

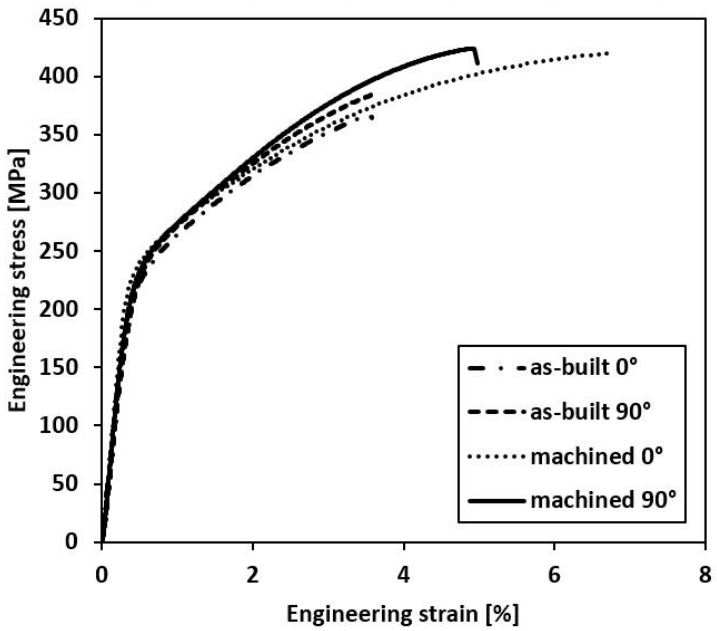

Fig. 3. Engineering stress-strain curve (room temperature testing).

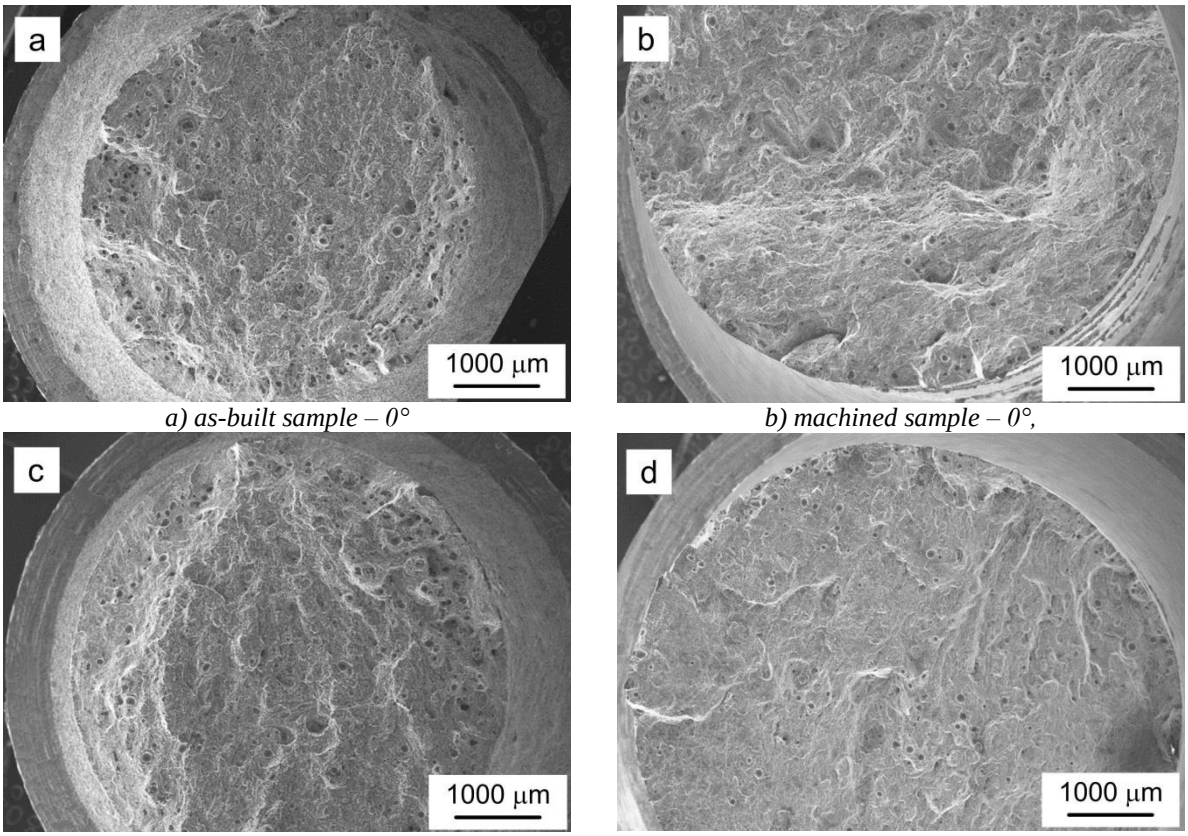

a) as-built sample – 0° *b) machined sample – 0°,*

c) as-built sample – 90° *d) machined sample – 90°*

Fig. 4. Fracture surface of specimens broken in tensile test – overview (SEM).

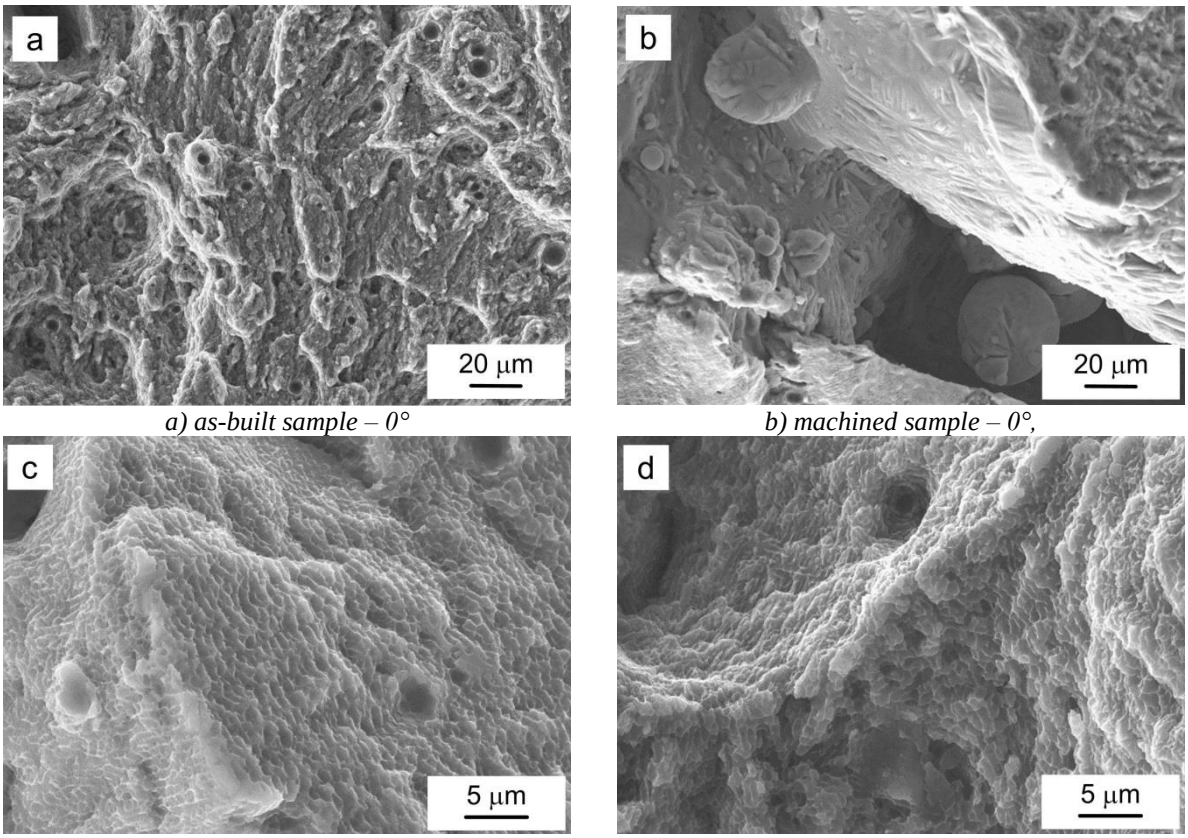

a) as-built sample – 0° *b) machined sample – 0°,*

c) as-built sample – 90° *d) machined sample – 90°*

Fig. 5. Fracture surface of specimens broken in tensile test – detail (SEM).

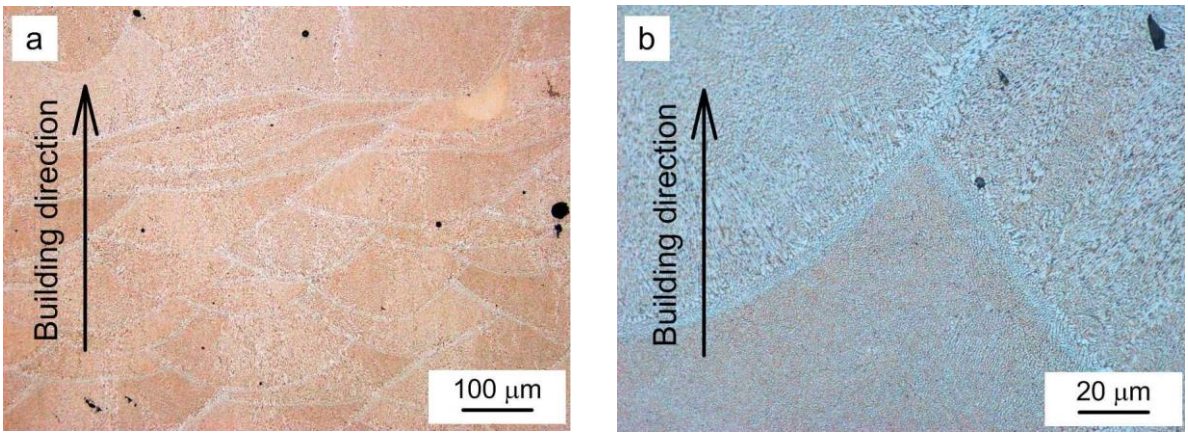

a) fish scale pattern *b) detail of fusion boundaries*

Fig. 6. Microstructure of SLM material at different magnification, longitudinal (X-Z) plane (LM).
(full colour version available online)

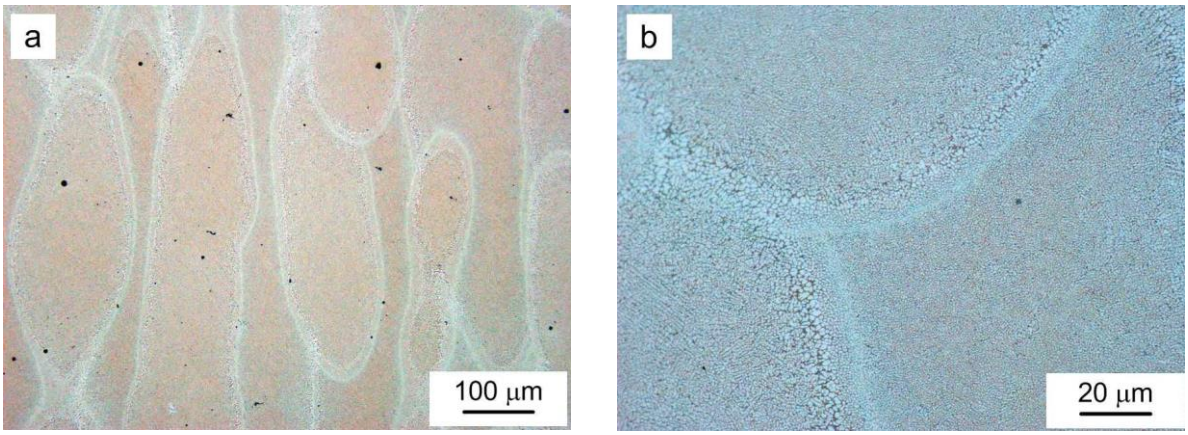

a) elongated SLM cells *b) detail of fusion boundaries*

Fig. 7. Microstructure of SLM material at different magnification, transverse (X-Y) plane (LM).
(full colour version available online)

A fractographic analysis of the samples broken during tensile tests was performed (Figs. 4 and 5). The fracture surface of all samples was rugged, with numerous gas porosity type inhomogeneities (Figs. 4 and 5a). Cavities with non-molten powder particles were also locally observed (lack of fusion porosity, Fig. 5b). The distribution of spherical pores was rather random over the whole cross-section of machined samples, compared with concentric circles of pores mostly in the subsurface layer of as-built samples (both building orientations), Fig. 4. In the central area of the cross-sections of as-built samples, pores were distributed rather randomly and in a lower amount (Figs. 4a, c). The fracture mechanism was of ductile character in all cases with small-dimple morphology, which indicates low energetic fracture (Figs. 5c, d).

Figs. 6 and 7 show the microstructure of SLM processed samples at various magnifications. Pores of different types are visible in the microstructure (gas pores and pores originating due to lack of fusion). The microstructure consists of single welds (SLM cells) separated by fusion boundaries; these cells and fusion boundaries are formed from solid solution α and fine particles of eutectic Si, respectively (Figs. 6 and 7). In the direction parallel to the building direction, a typical pattern of fish scale can be seen (Fig. 6), with the average interlayer melt pool depth (Fig. 6) being 90 μm. In the perpendicular section to the building direction, overlapping of laser track is clearly visible, with well-defined scan contours of SLM

cells (Fig. 7). This specific microstructure of elongated cells with dimensions exceeding hundreds of microns is given by the scanning strategy used.

4. Discussion

According to the results of the complex analyses performed, both 0.2% proof stress and UTS are independent of the building orientation [15], which affects only the elongation of analysed material. The elongation of machined samples built at a building angle of 0° was 38 % higher compared with samples built at a building angle of 90°. As-built samples exhibited smaller differences, with just 25 % higher elongation of samples with 0° building angle compared with samples with 90° building angle. An increase in elongation of AlSi10Mg alloy, dependent on the building angle, was also observed in [15] and [17]. The processing parameters used in [15] were different, compared with the present work: lower laser power (Lp = 200 W) and higher scan speed (Ls = 1400 mm/s) while in [17] the processing parameters were comparable with the present work, with the exception of heating the building platform to a higher temperature (200 °C) and an almost 2.5× higher hatch distance (Hd = 420 μm). The slight differences in mechanical properties obtained by the authors therefore should be linked to the differences mentioned above.

The surface quality of SLM processed samples had no significant influence on 0.2% proof stress in contrast to UTS and elongation. UTS increased by 11 % in machined samples (both building directions), and elongation increased by 47 % (0° orientation) and 36 % (90° orientation), respectively. According to the fractographic analysis (Figs. 4 and 5) the level of porosity was different in as-built and machined samples, especially in the subsurface layer. It can be assumed that the higher mechanical properties of machined samples (both orientations) are reached owing to the lower amount of microstructural defects (subsurface porosity is removed during machining) and so the matrix of material is not weakened by pore occurrence as in the case of as-built samples [19]. All observed mechanical properties of both as-built and machined samples prepared by SLM are higher compared with conventionally cast material (UTS 2.5× higher, elongation 2× higher) [20].

In contrast to the SLM processing parameters it seems that orientation of sample has no significant influence on yield strength and UTS (in agreement with [15, 17] as well) contrary to [21] where yield strength of samples with 0° orientation was markedly higher than for 90° orientation. This divergence is probably caused by different total volume of SLM processed material from which tensile test samples were made of.

5. Conclusion

AlSi10Mg alloy processed by SLM technology exhibits an inhomogeneous cellular microstructure with inhomogeneities of the type of gas-induced and lack-of-fusion porosity.

0.2% proof stress and UTS are not significantly affected by the building orientation unlike elongation, which is significantly higher in the case of 0° orientation.

Surface quality and subsurface porosity significantly affect tensile strength and elongation, when the material with higher surface quality achieved approx. 420 MPa UTS compared with 376 MPa UTS, and about half the elongation of the material with lower surface quality (as-built state).

Acknowledgements

This work has been supported by the European Regional Development Fund in the framework of the research project NETME Centre under the Operational Program Research and Development for Innovation No. CZ.1.5/2.1.00/01.002, and within the project NETME plus (Lo1202), project of Ministry of Education, Youth and Sports under the "national sustainability programme".

References

[1] D.D. Gu, W. Mainers, K. Wissenbach, R. Poprawe: Int. Mater. Rev. 57(3) (2012) 133–164.

[2] E. Louvis, P. Fox, Ch. J. Sutcliffe: J. Mater. Process. Tech. 211 (2011) 275–284.

[3] E. O. Olakanmi, R. F. Cochrane, K. W. Dalgarno: Prog. Mater. Sci. 74 (2015) 401–477.

[4] S. Siddique, M. Imran, E. Wycisk, C. Emmelmann: J. Mater. Process. Tech. 221 (2015) 205–213.

[5] N. Read, W. Wang, K. Essa, M. M. Attallah: Materials and Design 65 (2015) 417–424.

[6] W. J. Sames, F. A. List, S. Pannala, R. R. Dehoff, S. S. Babu: Int. Mater. Rev. 61(5) (2016) 315–360.

[7] N. T. Aboulkhair, N. M. Everitt, I. Ashcroft, C. Tuck: Additive Manufacturing 1–4 (2014) 77–86.

[8] Ch. Weingarten, D. Buchbinder, N. Pirch, W. Meiners, K. Wissenbach, R. Poprawe: J. Mater. Process. Tech. 221 (2015) 112–120.

[9] F. Trevisan, F. Calignano, M. Lorusso, J. Pakkanen, A. Aversa, E. P. Ambrosio, M. Lombardi, P. Fino, D. Manfredi: Materials 10 (2017) 1–23.

[10] B. Vrancken, R. Wauthle, J. P. Kruth, J. Van Humbeeck: Proc. 24th Int Solid Free Fabr Symp (2013) 393–407.

Y. Liu, Y. Yang, D. Wang: Int. J. Adv. Manuf. Technol 90 (2017) 2913–2923

[11] X. Cao, W. Wallace, J. P. Immarigeon, C. Poon: Mater. Manuf. Process. 18(1) (2003) 23–49.

[12] R. Liu, Z. Dong, Y. Pan: Trans. Nonferrous Met. Soc. China 16 (2006) 110–116.

[13] L. Pantělejev, D. Koutný, D. Paloušek, J. Kaiser: Mater. Sci. Forum 891 (2016) 343-349.

[14] K. Kempen, L. Thijs, J. Van Humbeeck, J.-P. Kruth: Physics Procedia 39 (2012) 439–446.

[15] L. Thijs, K. Kempen, J.-P. Kruth, J. Van Humbeeck: Acta Materialia 61 (2013) 1809–1819.

[16] L. Hitzler, Ch. Janousch, J. Schanz, M. Merkel, B. Heine, F. Mack, W. Hall, A. Öchsner: J. Mater. Process. Tech. 243 (2017) 48–61.

[17] I. Rosenthal, A. Stern, N. Frage: Mat. Sci. Eng. A682 (2017) 509–517.

[18] U. Tradowsky, J. White, R. M. Ward, N. Read, W. Reimers, M. M. Attallah: Materials and Design 105 (2016) 212–222.

[19] N. T. Aboulkhair, I. Maskery, Ch. Tuck, I. Ashcroft, N. M. Everit: Mat. Sci. Eng. A667 (2016) 139–146.

[20] N. Takata, H. Kodaira, K. Sekizawa, A. Suzuki, M. Kobashi: Mat. Sci. Eng. A704 (2017) 218–228.